

## Characterization of ZnSe microspheres synthesized under different hydrothermal conditions

Yu-lu DUAN<sup>1</sup>, Sheng-lian YAO<sup>1</sup>, Cheng DAI<sup>1</sup>, Xiao-he LIU<sup>2</sup>, Guo-fu XU<sup>1,3</sup>

1. School of Materials Science and Engineering, Central South University, Changsha 410083, China;

2. School of Minerals Processing and Bioengineering, Central South University, Changsha 410083, China;

3. Key Laboratory of Nonferrous Materials Science and Engineering of Ministry of Education, Central South University, Changsha 410083, China

Received 29 July 2013; accepted 16 January 2014

**Abstract:** ZnSe microspheres were synthesized via a facile hydrothermal method under mild conditions using aqueous zinc nitrate and sodium selenite as raw materials. The effects of hydrothermal temperature, reaction time, concentration of NaOH and amount of hydrazine hydrate on the phase structure, morphology and size of final products were carefully investigated. The phase structures, morphologies and optical properties of the final products were characterized by X-ray diffraction (XRD), scanning electron microscopy (SEM), transmission electron microscopy (TEM) and photoluminescence (PL) spectroscopy. ZnSe microspheres assembled by average size (about 20 nm) nanocrystals were prepared using 20 mL of 1 mol/L NaOH solution and 10 mL of hydrazine hydrate at 180 °C for 4 h. The results show that the products obtained at low hydrothermal temperature and short reaction time have poor crystallinity and contain impurity phases. The appropriate NaOH concentration and amount of hydrazine hydrate ensure to obtain pure ZnSe with spherical morphology and better luminescence property.

**Key words:** ZnSe microsphere; nanocrystal; hydrothermal method; luminescence property

### 1 Introduction

During the past decades, wide band gap semiconductor materials have attracted considerable attention due to their size-dependent properties and important technological applications [1,2]. Of the various II–VI semiconductors, zinc selenide (ZnSe) with a direct band gap of 2.70 eV (460 nm) is especially interesting because it is widely used for various applications [3], such as nonlinear optical devices [4], displays [5], sensors [6] and infrared windows [7]. Nanostructure of the photocatalytic materials can be considered a primarily promising strategy to gain factorial enhancements in photocatalyst due to both higher surface-to-volume ratios and higher redox potentials with an increase in band gap energy as a result of the so-called quantum size effect [8,9]. ZnSe has long been a material of choice of blue diode lasers and photovoltaic solar cells [10,11]. Efforts in the preparation of ZnSe usually focused on the synthesis of ZnSe nanocrystals with luminescent properties from single-molecular precursors

[12,13]. Recently, many efforts have been devoted to the synthesis of spherical ZnSe semiconductors. XIONG et al [14] synthesized ZnSe nanobelts with high photocatalytic activity in the degradation of fuchsine and solution under UV light irradiation through a solvothermal approach. But the most important challenges in materials is to control the structure of materials on specific nanomorphologies [15,16].

Many new methods have been investigated to prepare ZnSe, including a variety of colloids and composite particles [17]. CAO et al [18] presented a simple hydrothermal route for the synthesis of wurtzite 3D flowerlike ZnSe nanostructures in high yield by a complex hydrothermal treatment using ethylenediamine-tetraacetic acid (EDTA). But most of the synthesis general involved intricate processing. To the best of our knowledge, no further studies have been reported on the synthesis of ZnSe nanostructures without any other organic additives (like ethylenediaminetetraacetic acid) although they are strongly desired. And the effects of the experiment parameters, such as concentration of NaOH, amount of hydrazine hydrate, reaction time, and

temperature, on the evolution of ZnSe microspheres morphology and structure have not been reported detailedly. Therefore, the development of simple template-free and facile methods for the preparation of ZnSe microspheres with intrinsic optical properties still maintains a highly challenge. Here, ZnSe microspheres have been successfully synthesized via a facile hydrothermal method under mild conditions using aqueous zinc nitrate and sodium selenite as zinc and selenium source, sodium hydroxide as precipitating reagent and hydrazine hydrate as both alkaline and complexing reagent. The effects of hydrothermal temperature, reaction time, concentration of NaOH and amount of hydrazine hydrate on the phase structure, morphology and size of final products have been carefully investigated. The phase structures, morphologies and optical properties of the final products were characterized by means of X-ray diffraction (XRD), scanning electron microscopy (SEM), transmission electron microscopy (TEM) and photoluminescence (PL) spectroscopy.

## 2 Experimental

All chemical solvents and reagents used in this work, such as aqueous zinc nitrate ( $\text{Zn}(\text{NO}_3)_2 \cdot 6\text{H}_2\text{O}$ ), sodium selenite ( $\text{Na}_2\text{SeO}_3$ ), sodium hydroxide (NaOH) and hydrazine hydrate ( $\text{N}_2\text{H}_4 \cdot \text{H}_2\text{O}$ ), were of analytical grade and used without any further purification. Deionized water was used in all preparations.

In a typical procedure, 0.298 g of  $\text{Zn}(\text{NO}_3)_2 \cdot 6\text{H}_2\text{O}$  and 0.173 g of  $\text{Na}_2\text{SeO}_3$  were added into a Teflon-lined stainless steel autoclave of 50 mL capacity and dissolved in 20 mL of 1 mol/L NaOH solution through supersonic vibration. Then 10 mL of hydrazine hydrate (80% v/v) solution was added dropwise during vigorous stirring. Next, 10 mL of deionized water was added into the autoclave that was filled up to 80% of the total volume. After 10 min stirring, the autoclave was sealed and maintained at 180 °C for 4 h. Subsequently, the system was allowed to cool to the room temperature naturally. The resulting precipitate was collected by centrifugal sedimentation, washed with absolute ethanol and distilled water in sequence several times. The final product was dried at 60 °C for 8 h.

The obtained products were characterized by a Rigaku D/MAX2500 X-ray diffractometer (XRD) with  $\text{Cu K}_\alpha$  radiation ( $\lambda=0.154051$  nm). The operation voltage and current were kept at 40 kV and 40 mA, respectively. The size and morphology of the as-synthesized products were determined at 10 kV by a Sirion 200 field emission scanning electron microscope (SEM) and at 200 kV by a Tecnai G<sup>2</sup> 20ST transmission electron microscope (TEM)

and a JEOL JEM-2100F high-resolution transmission electron microscope (HRTEM). Energy-dispersive X-ray spectroscopy (EDS) was taken on the SEM. The room-temperature photoluminescence (PL) measurement was carried out on an F-4500 spectrophotometer using the 329 nm excitation line of Xe light.

## 3 Results and discussion

### 3.1 Morphology and structure

The crystal structure of the ZnSe microspheres prepared using 20 mL of 1 mol/L NaOH solution and 10 mL of hydrazine hydrate at 180 °C for 4 h were investigated by XRD. Figure 1 shows a typical XRD pattern of ZnSe precursors, in which all the diffraction peaks can be well indexed to cubic ZnSe with lattice constant  $a=0.567$  nm, which is in good agreement with the standard PDF data (37–1463).

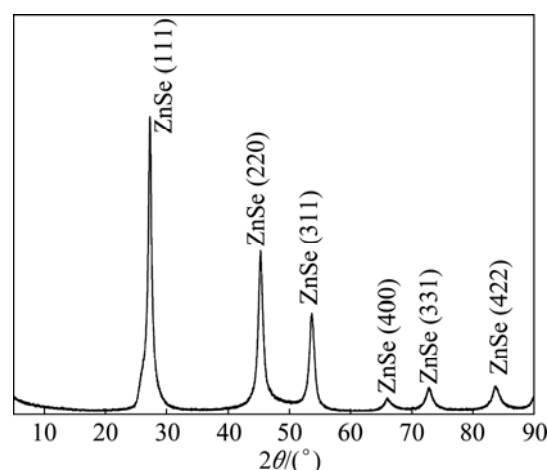


**Fig. 1** XRD pattern of as-prepared ZnSe products using 20 mL of 1 mol/L NaOH solution and 10 mL of hydrazine hydrate at 180 °C for 4 h

Figure 2 shows the morphology, phase structure, and size of ZnSe microspheres prepared using 20 mL of 1 mol/L NaOH solution and 10 mL of hydrazine hydrate at 180 °C for 4 h. As shown in Fig. 2(a), the diameter of ZnSe spheres is in the range of 1–3  $\mu\text{m}$ . Figure 2(b) shows an individual broken ZnSe microsphere assembled by uniform nanocrystals with the size of about 20 nm from inside to outside. SAED pattern of as-prepared ZnSe microspheres could be indexed to pure cubic ZnSe (Fig. 2(c)), which suggests that those microspheres are polycrystalline. Further investigations of the ZnSe nanocrystals come from the HRTEM analyses (Fig. 2(d)). The legible spacing was calculated to be about 0.328 nm, which is in good agreement with the (111) plane of face-centered cubic ZnSe.

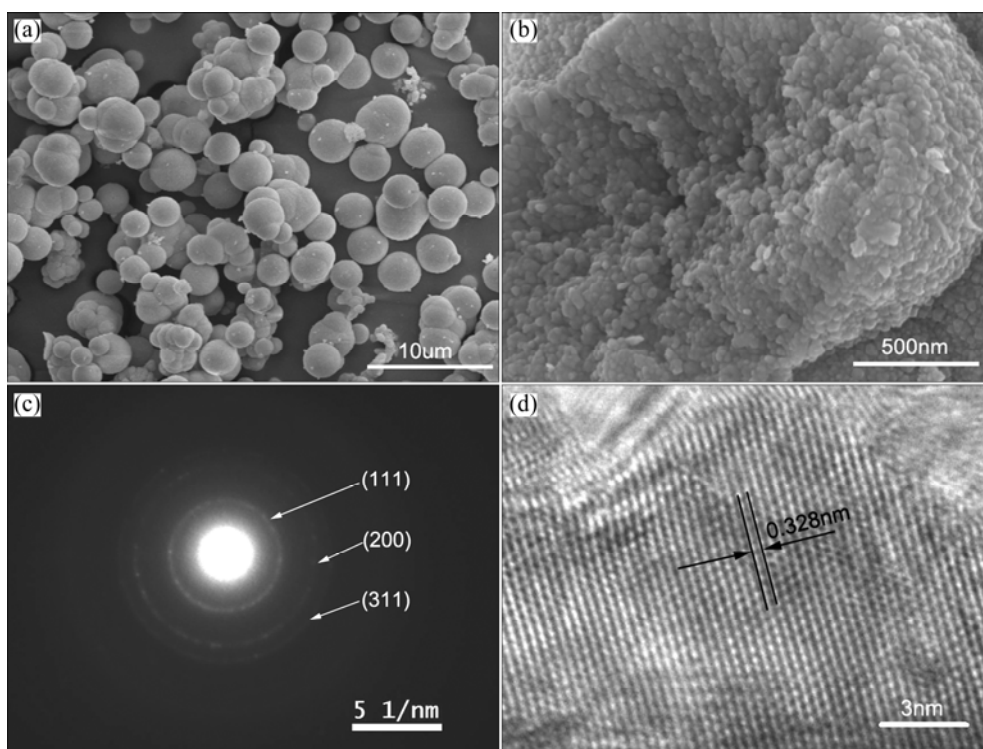


**Fig. 2** SEM images (a, b), SAED pattern (c), HRTEM image (d) of as-prepared ZnSe products using 20 mL of 1 mol/L NaOH solution and 10 mL of hydrazine hydrate at 180 °C for 4 h

### 3.2 Effect of reaction conditions on growth of ZnSe

Furthermore, further researches suggested that hydrothermal temperature, reaction time, concentration of NaOH and amount of hydrazine hydrate had effect on the phase structures, size and morphology of ZnSe microstructures.

Figure 3 shows the XRD patterns of the samples prepared at 100, 140, 180 and 220 °C without other condition changed. The obvious reflections of the XRD patterns could be indexed to cubic zinc blende structure ZnSe (PDF database No: 37–1463). With the elevation of hydrothermal temperature, the diffraction peaks become

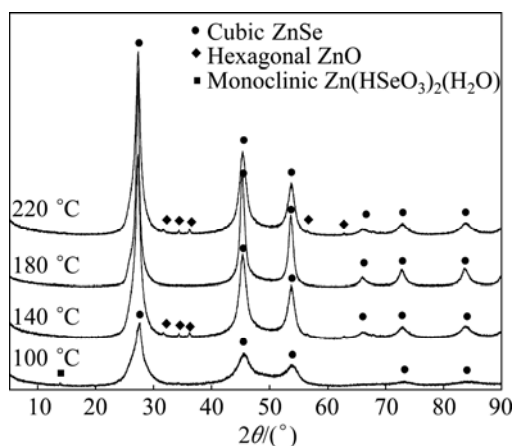


**Fig. 3** XRD patterns of products obtained without other condition changed at 100, 140, 180 and 220 °C

higher and far narrower, implying that the crystallinity of products is continuously improved. The sample prepared at 180 °C shows the highest crystallinity, while the samples prepared at lower hydrothermal temperature (100 °C, 140 °C) show poor crystallinity. In addition, the monoclinic  $\text{Zn}(\text{HSeO}_3)_2(\text{H}_2\text{O})$  can be found in the XRD pattern of as-prepared products obtained at 100 °C. And the small amount of hexagonal ZnO can be obtained at 140 °C and 220 °C without other condition changed. The above results indicate that higher temperature (180 °C) is propitious to generate the pure phase of cubic ZnSe.

Figures 4(a) and (b) show the SEM images of the ZnSe microstructures obtained at 100 °C, 140 °C without other condition changed, suggesting that the main products are microspheres with diameters in the range of 1–5 μm. Compared with the products synthesized at 180 °C (Fig. 2(a)), lamellate particles and more small size (<1 μm) microspheres products can be observed at 100 °C and 140 °C. And the average diameter of microspheres obtained at low hydrothermal temperature (100 °C) is bigger than those obtained at high temperature (140 °C and 180 °C). Moreover, Figs. 4(c) and (d) show that the average size and crystallinity of ZnSe nanocrystal on the surface of microsphere gradually increase with the elevation of hydrothermal temperature. And the morphology of ZnSe nanocrystal on the surface of microsphere developed from subsphaeroidal to cubic shape. The reason may be that

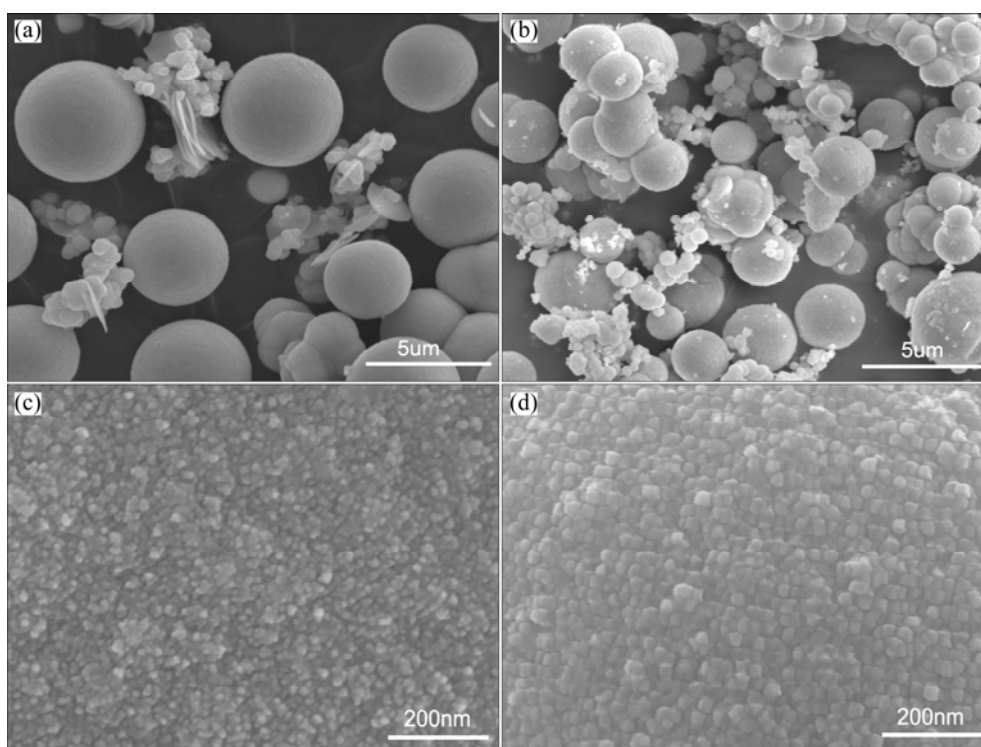


**Fig. 4** SEM images of ZnSe microstructures obtained at different hydrothermal temperatures: (a), (c) 100 °C; (b), (d) 140 °C

there is not enough energy to the growth of ZnSe nanocrystal at low temperature. And spherical particle has the lower surface energy than cubic particle. Therefore, the morphology of ZnSe nanocrystal would become subsphaeroidal, and it would become cubic at high temperature. The effect of the temperature field at high temperature may be more intense than at low temperature. The microsphere would be broken, and the size of microsphere became smaller at high temperature. Many small pieces are shown in Fig. 4(b), while few small pieces are found in Fig. 4(a).

To sum up, the hydrothermal temperature had little effect on morphology of final products. But it had influence on the phase structure and the size of final products.

The effects of reaction time on the phase structures, size and morphology of ZnSe microstructures were further investigated. Figure 5 shows the XRD patterns of the products that were synthesized using 20 mL of 1 mol/L NaOH solution and 10 mL hydrazine hydrate at 180 °C for 2 h, 4 h, 8 h and 24 h, respectively. All the peaks of XRD patterns could be indexed to cubic zinc blende structure ZnSe. With the elongation of reaction time, the diffraction peaks become higher and far narrower, indicating that the crystallinity of products is continuously improved and the grain size of the products increases. When the reaction time is elongated to 24 h, the XRD pattern is close to the shorter reaction time in the low angle, but has a shift to high angle. This indicates

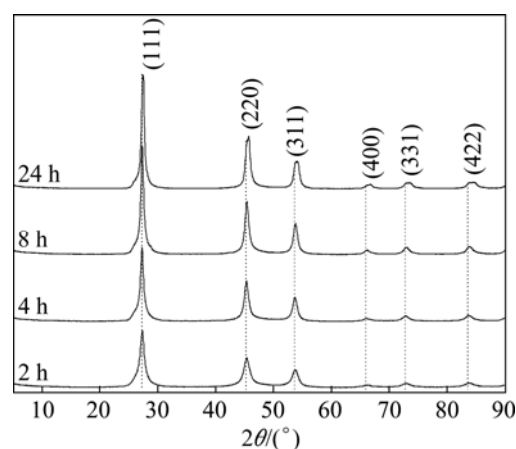


**Fig. 5** XRD patterns of products prepared at 180 °C for different time using 20 mL of 1 mol/L NaOH solution and 10 mL of hydrazine hydrate

that two kinds of products have been prepared with 24 h. One is the same with the product of shorter reaction time, and the other has the same crystal structure with the former but the lattice constant changed. According to the diffraction formula,  $2d\sin\theta=\lambda$ , the lattice constant of the other product is reducible.

Low magnification SEM images of ZnSe obtained at 180 °C for 2 h, 8 h and 24 h are shown in Figs. 6(a), (b) and (c), respectively. Compared with the SEM image of the products in Fig. 2(a), the size of ZnSe microspheres did not grow up with the reaction time extending. A large number of small size (<1 μm) microspheres can be observed in Fig. 6(a), which indicates that short reaction

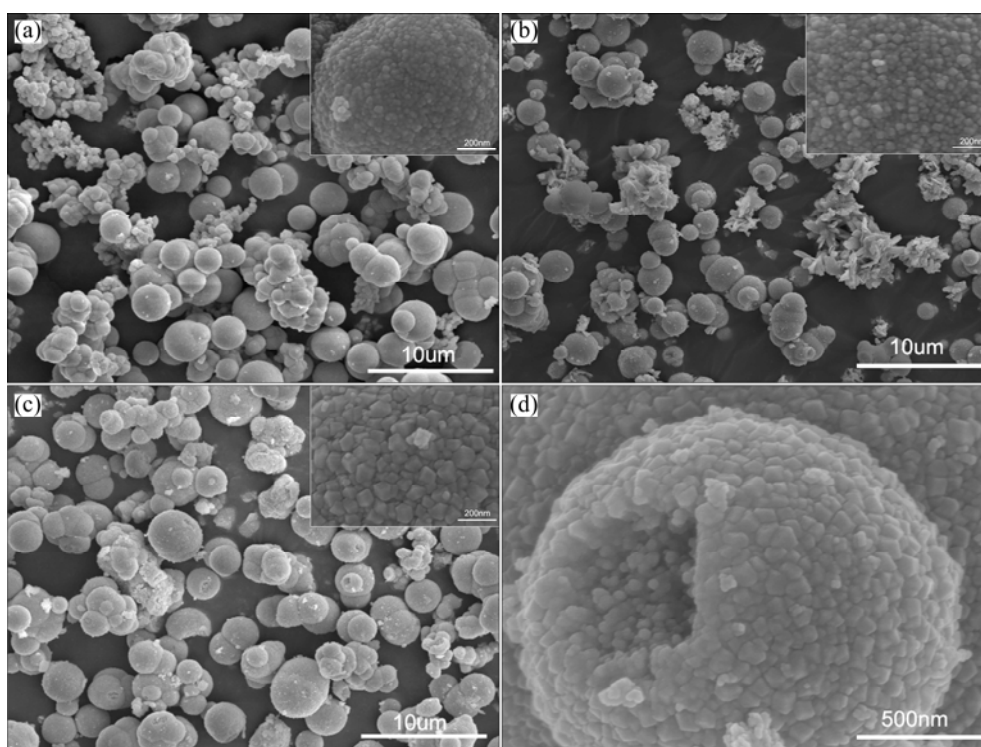


**Fig. 6** SEM images of products obtained at 180 °C for different reaction time: (a) 2 h; (b) 8 h; (c), (d) 24 h

time leads to more small size microspheres. Figure 6(b) shows a typical SEM image of the as-prepared ZnSe obtained at 180 °C for 8 h. It is obvious that lamellate particles can be observed except microspheres. When the reaction time is elongated to 24 h, the morphology of products is mainly sphere in Fig. 6(c). But SEM image of an individual broken microsphere of products obtained for 24 h (Fig. 6(d)) gives more detail difference from the products obtained for 4 h (Fig. 2(b)). The inside of ZnSe microspheres is subsphaeroidal, while the ZnSe nanocrystals on the surface of microsphere are cubic. The insets of Fig. 6(a), 6(b) and 6(c) show that ZnSe nanocrystals on the surface of microspheres were prepared for 2 h, 8 h and 24 h, respectively. The size of ZnSe nanocrystals enlarges with the reaction time increasing, especially the 24 h. Moreover, with the reaction time increasing, the shape of ZnSe nanocrystals gradually changed from subsphaeroidal to cubic ones.

Therefore, long reaction time does not make ZnSe microspheres enlarge obviously, but the ZnSe nanocrystals on the surface of microsphere evolve from subsphaeroidal to larger cubic particle. So, the ZnSe microspheres assembled by uniform size nanocrystals can be synthesized with longer reaction time, and this kind of product could lead to different performance. In addition, we had known that reaction time had effects on the size of final products, while it had little influence on the phase structure and morphology of final products.

The sodium hydroxide concentration is another important factor that determines the morphology of final products. The products were obtained at 180 °C for 4 h, using 10 mL of hydrazine hydrate and 20 mL of water, 20 mL of 0.25 mol/L, 0.5 mol/L, 1 mol/L NaOH solutions, respectively. Figure 7(a) shows the typical SEM image of products prepared in the absence of NaOH. It is obviously observed that the spherical particles could not be synthesized when NaOH was absent. When the concentration of NaOH was about 0.25 mol/L, the products are composed of microspheres with a mean diameter of about 1.5 μm, as shown in Fig. 7(b). Also, many flower-like particles can be observed. If the concentration of NaOH was strengthened up to 0.5 mol/L, the as-prepared products were mainly composed of microspheres with a mean diameter of about 2 μm and few flower-like particles (Fig. 7(c)). Detailed results show that the as-prepared products obtained using 0.25 mol/L NaOH contain more flower-like particles than those using 0.5 mol/L NaOH. As seen in Figs. 7(a), (b), (c) and Fig. 2(a) (1 mol/L), with the NaOH concentration decreasing, the sizes of microspheres reduce, and non-spherical particles appear.

EDS analysis was also carried out on the chemical composition of the spherical and flower-like particles. The results show that the spherical particles are composed of Se and Zn (Fig. 8(a)), and the flower-like particles mainly consist of O and Zn (Fig. 8(b)), which agrees well with the XRD patterns.

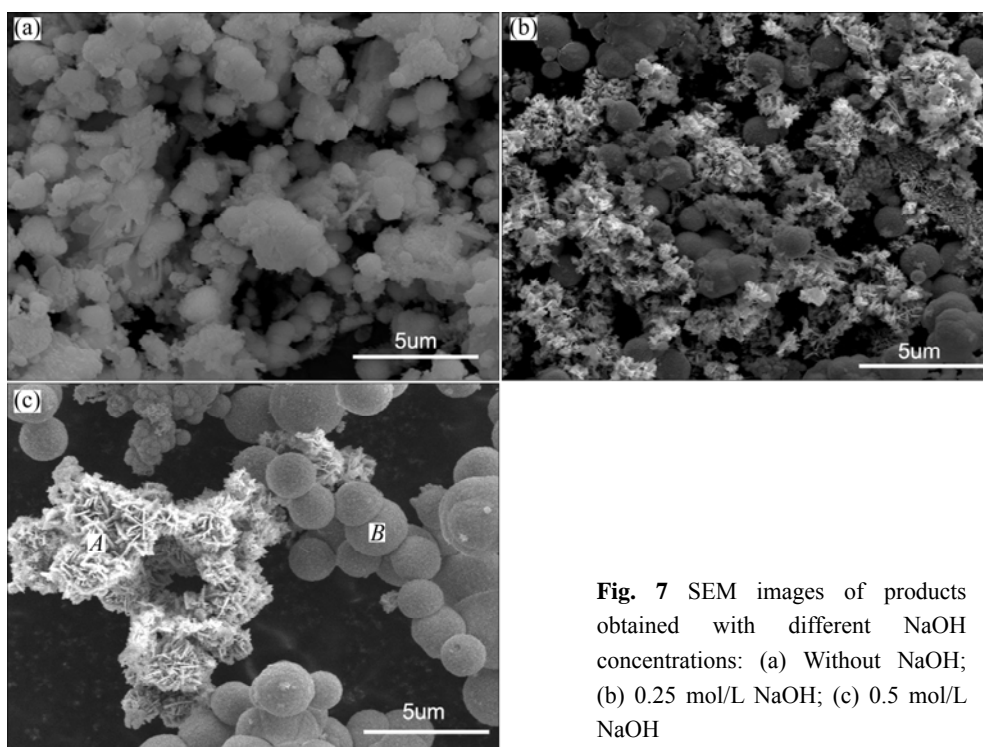


**Fig. 7** SEM images of products obtained with different NaOH concentrations: (a) Without NaOH; (b) 0.25 mol/L NaOH; (c) 0.5 mol/L NaOH

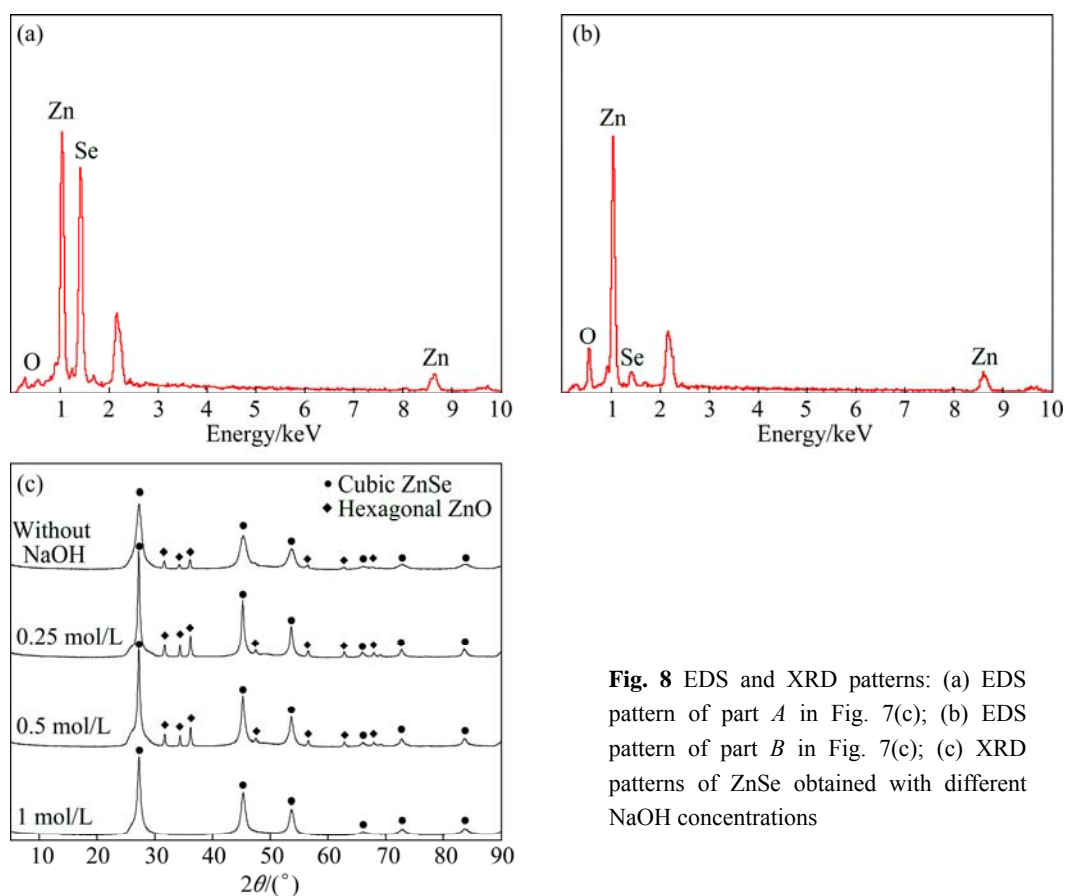
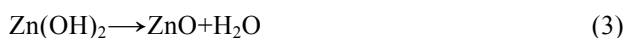
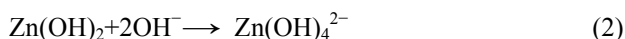


**Fig. 8** EDS and XRD patterns: (a) EDS pattern of part *A* in Fig. 7(c); (b) EDS pattern of part *B* in Fig. 7(c); (c) XRD patterns of ZnSe obtained with different NaOH concentrations

As seen in Fig. 8(c), the XRD pattern of the product obtained with 1 mol/L NaOH can be only indexed to cubic ZnSe. Moreover, with the reduction of sodium hydroxide concentration (0.5 mol/L, 0.25 mol/L and 0

mol/L), the diffraction peaks of hexagonal ZnO become stronger and broaden, implying that the size of product particles is smaller than the former groups. All the phenomena can be explained by the following chemical

reactions.



Amphoteric hydroxide  $\text{Zn}(\text{OH})_2$  can dissolve in bountiful  $\text{OH}^-$  solution, so the  $\text{Zn}^{2+}$  participates in the main reaction to synthesize the goal product  $\text{ZnSe}$ . Or  $\text{Zn}(\text{OH})_2$  deposit could lose  $\text{H}_2\text{O}$ , leading to the appearance of  $\text{ZnO}$ .

So, the  $\text{NaOH}$  concentration plays an important role in controlling the morphology of products. The evolution of products synthesized with different concentrations of  $\text{NaOH}$  clearly indicates that  $\text{NaOH}$  plays a key role in the formation of  $\text{ZnSe}$  microstructures and proper amount of  $\text{NaOH}$  is crucial for the formation of  $\text{ZnSe}$  microspheres while keeping the self-assembly structures of final products.

Furthermore, the influence of amount of hydrazine hydrate on morphology of final products was also investigated. Figure 9 shows the XRD patterns of products obtained at  $180^\circ\text{C}$  for 4 h, using different amount of hydrazine hydrate (0, 10 mL and 20 mL). The XRD pattern of the as-prepared product in the absence of hydrazine monohydrate can be indexed to hexagonal  $\text{ZnO}$ . And no characteristic peaks of other impurities can be detected. When the amount of hydrazine hydrate was about 10 mL, the product can be indexed to only cubic

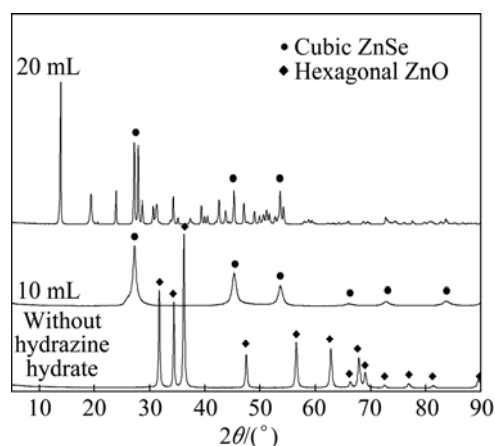


**Fig. 9** XRD patterns of products obtained at  $180^\circ\text{C}$  for 4 h, using 20 mL of 1 mol/L  $\text{NaOH}$  solution and different volumes of hydrazine hydrate (0, 10 mL and 20 mL)

$\text{ZnSe}$ . However, when 20 mL hydrazine monohydrate was added in the synthesis system, the XRD pattern of the product can be indexed to the cubic  $\text{ZnSe}$  and other impurities. The XRD result illustrates that the apposite amount of hydrazine monohydrate also plays an important role in the synthesis of pure cubic  $\text{ZnSe}$ .

Figure 10(a) shows a typical SEM image of the as-prepared product obtained in the absence of hydrazine monohydrate. Many multifarious form particles are observed, which are composed of lamellate and

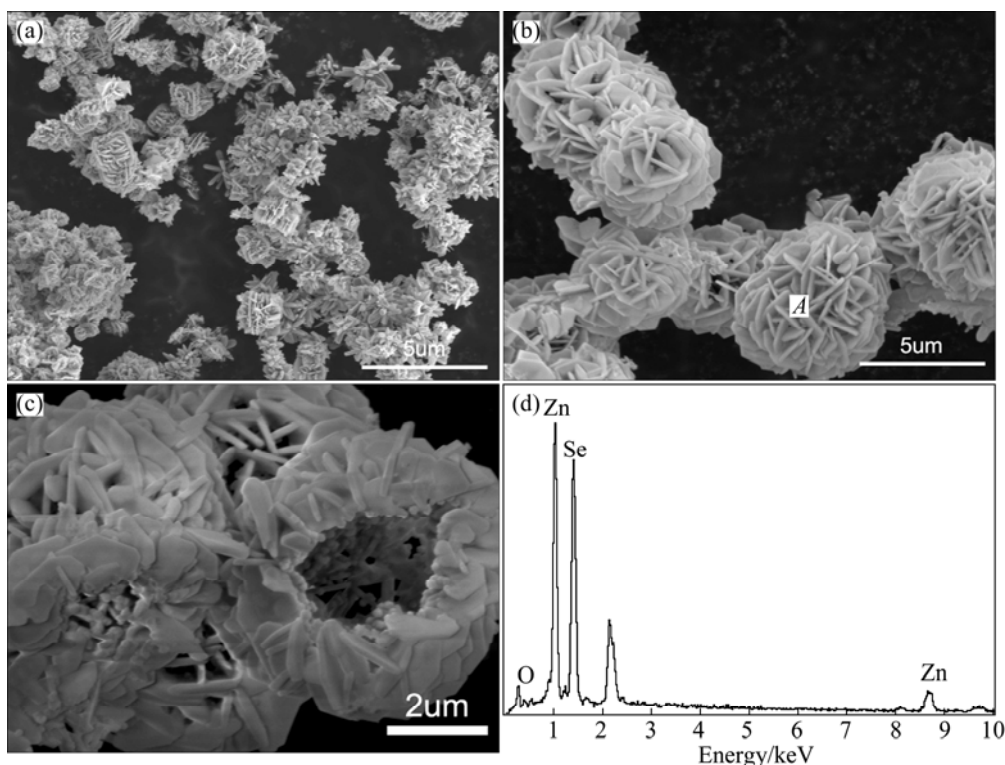
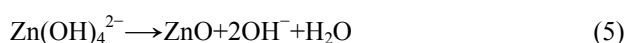
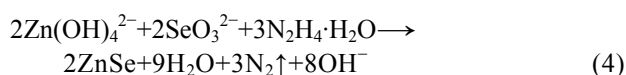


**Fig. 10** SEM images and EDS pattern of products obtained at  $180^\circ\text{C}$  for 4 h, using 20 mL of 1 mol/L  $\text{NaOH}$  solution and different volumes of hydrazine hydrate: (a) SEM, without  $\text{N}_2\text{H}_4\cdot\text{H}_2\text{O}$ ; (b), (c) SEM, 20 mL  $\text{N}_2\text{H}_4\cdot\text{H}_2\text{O}$ ; (d) EDS pattern of part A in (b)



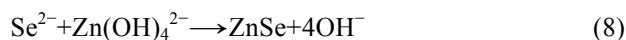
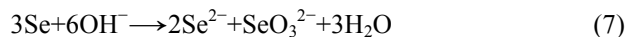
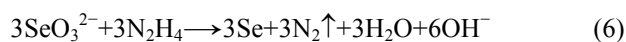
baculiform ZnO. As seen in Fig. 10(b), beautiful particles are observed, when the products were synthesized using 20 mL of hydrazine monohydrate. Figure 10(c) shows the higher magnification SEM image of the product prepared with 20 mL of hydrazine monohydrate, indicating that the particles are microspheres composed of lamellate grains. Because the phase structures of product obtained with 20 mL of hydrazine monohydrate cannot be explained by XRD, EDS analysis was also carried out on the chemical composition of this product, and the result is shown in Fig. 10(d). The result reveals the elements of the product are Zn, Se and marginal O. So, the excessive hydrazine monohydrate added into the reaction system may lead to extraneous O into the product.

According to the results of XRD, SEM and EDS, hydrazine monohydrate as a strong alkaline reducing agent plays an important role in regulating the morphology and controlling the phase composition of product. The XRD pattern of product in the absence of hydrazine monohydrate can be only indexed to hexagonal ZnO, indicating that if there is not reducing atmosphere offered by hydrazine monohydrate,  $\text{Se}^{4+}$  cannot be reduced to  $\text{Se}^{2-}$  and attend the following reaction Eq. (4) with  $\text{Zn}^{2+}$  to synthesize the product ZnSe. So, ZnO would be produced according to chemical reaction Eq. (5) [2]. But when enough hydrazine monohydrate (20 mL) was added in the synthesis system, the products would contain other impurities except the cubic ZnSe, corresponding to the unknown peaks in the XRD patterns. Therefore, hydrazine monohydrate as a strong alkaline reducing agent plays an important role in regulating the morphology and controlling the phase composition of product. The appropriate amount of hydrazine hydrate ensures that the final products are pure ZnSe with spherical morphology. And we believe that the interaction between inorganic materials and hydrazine monohydrate may be the main driving force for the formation of a flowerlike structure.



The reactions to form ZnSe nanostructures can be

formulated as follows:



According to the literature, Se and  $\text{Na}_2\text{SeO}_3$  are the frequently used selenium sources in the solution preparation of ZnSe.  $\text{Na}_2\text{SeO}_3$  is used instead of Se powder in our reaction because it can dissolve easily in water and be reduced to highly reactive Se quickly by hydrazine hydrate upon heating. These highly reactive ultrafine Se particles are produced in situ form  $\text{Se}^{2-}$  much easier than commercial Se powders. Furthermore, Se powders cannot dissolve into the solution completely, the synthetic reactions are incomplete and the obtained sample contains an impurity of Se, which is not easy to eliminate from the products.

### 3.3 Photoluminescence spectrum of products

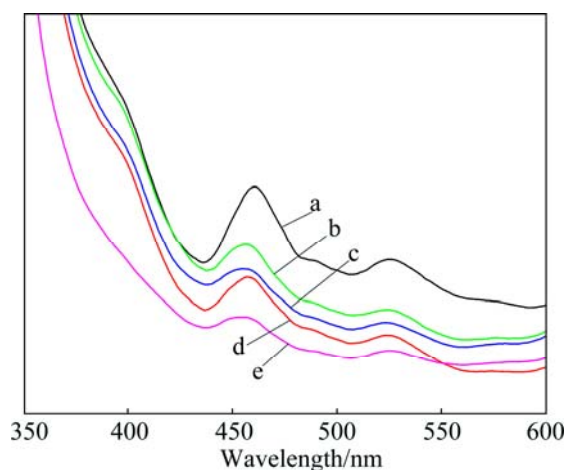
The as-prepared products with the different experiment parameters show different luminescence properties. Therefore, the room-temperature photoluminescence (PL) under the excitation wavelength of 329 nm has been performed to investigate the optical properties of the as-prepared products. Table 1 lists some as-prepared products with different experiment parameters.

Figure 11 presents the PL spectra of as-prepared products in the wavelength range of 350–600 nm. Both of the particles prepared with different experiment parameters exhibit the same blue and green emissions. Figure 11 presents the PL spectra of particles obtained with different experiment parameters, in which a broad, well-resolved peak located at ~450 nm was observed. The absorption peak is obviously blue shifted relative to the bulk one (460 nm) [19], and a band green emission with peak at 530 nm can be observed. The data of curves in Fig. 11(a) clearly indicate that the ZnSe flower-like particles photocatalysts show the highest luminescence property. The high luminescence property of ZnSe flower-like particles might be attributed to the following reasons: 1) Flower-like superstructure and mesopores in the leaves make them possess higher BET surface area

**Table 1** Some as-prepared products with different experiment parameters

No.	$n(\text{Zn}(\text{NO}_3)_2 \cdot 6\text{H}_2\text{O})/$ mol	$n(\text{Na}_2\text{SeO}_3)/$ mol	$c(\text{NaOH})/$ ( $\text{mol} \cdot \text{L}^{-1}$ )	$v(\text{N}_2\text{H}_4 \cdot \text{H}_2\text{O})/$ mL	$t/^\circ\text{C}$	$\tau/\text{h}$
a	0.001	0.001	1	10	140	4
b	0.001	0.001	0.25	10	180	8
c	0.001	0.001	0	10	180	24
d	0.001	0.001	1	10	180	4
e	0.001	0.001	1	20	180	4





**Fig. 11** PL spectra of particles obtained under different experiment parameters

than ZnSe microspheres, which results in an increase of adsorption percentages and benefits the enhancement of the luminescence property of ZnSe. 2) The energy of the band gap of ZnSe microspheres estimated from the main absorption edges of the UV-vis diffuse reflectance spectrum is 2.8 eV, which is slightly higher than the well-known band gap of 2.70 eV for bulk ZnSe due to the so-called quantum size effect. As known, the optimum band gap plays a major role in the photocatalytic activities of semiconductors. Electron hole pair generation is dependent on the band gap of ZnSe. The increase in band gap is useful in obtaining higher electron-hole pair generation. Therefore, the photocatalytic properties have been greatly improved [18]. The luminescence property of the as-prepared products with experiment parameters (b) and (c) are higher than others because the products constituted of the cubic ZnSe and hexagonal ZnO (Fig. 8(f)). As known, the luminescence property of hexagonal ZnO (band gap of 3.70 eV) is better than cubic ZnSe. So, hexagonal ZnO could increase the the luminescence property of the products. The luminescence property of the as-prepared ZnSe microspheres with experiment parameters (d) is lower than others. The blue emission originates from the excitonic recombination corresponding to the near-band edge emission of ZnSe, which may be attributed to the quantum-confined effect of the nanocrystals aggregating on the spheres [2]. The green luminescence can be attributed to the recombination of an electron and a photo-generated hole caused by surface defects [20–22]. The data of curves in Fig. 11(e) clearly indicate that the products obtained without hydrazine hydrate have the lowest photocatalytic activity. The phase consists of cubic ZnSe and other impurities (Fig. 9). Those impurities would decrease the luminescence property of the as-prepared ZnSe microspheres.

## 4 Conclusions

1) The products obtained at low hydrothermal temperature have poor crystallinity and contain impurities phases, the products obtained at the highest hydrothermal temperature (220 °C) also contain impurities phases, while the higher temperature (180 °C) is propitious to generate the pure phase of cubic ZnSe. And ZnSe nanocrystals synthesized at short reaction time have poor crystallinity. However, when reaction time is elongated, ZnSe nano-unit cell will have nonhomogeneity.

2) NaOH and hydrazine monohydrate play important role in the formation of ZnSe microstructures, controlling the phase composition, the morphology and the luminescence property of the product. A proper amount of NaOH is crucial for the formation of ZnSe microspheres.

3) ZnSe microspheres were synthesized using 20 mL of 1 mol/L NaOH solution and 10 mL of hydrazine hydrate at 180 °C for 4 h. The product has cubic zinc blende structure ZnSe microsphere assembled by uniform nanocrystals with average size of about 20 nm from inside to outside. And the PL results show that ZnSe microspheres have high PL emission properties.

## Acknowledgments

We are grateful to Dr. Xu LI for his constructive discussions and useful suggestions, also thanks to Ji-wu HUANG and Ju-fei CHEN for their assistance in XRD and SEM measurements.

## References

- [1] PENG Q, DONG Y J, LI Y D. ZnSe semiconductor hollow microspheres [J]. *Angewandte Chemie*, 2003, 42(26): 3027–3030.
- [2] WANG H N, DU F L. Hydrothermal synthesis of ZnSe hollow microspheres [J]. *Cryst Res Technol*, 2006, 41(4): 323–327.
- [3] HEULINGS-IV H R, HUANG X Y, LI J. Mn-substituted inorganic-organic hybrid materials based on ZnSe: nanostructures that may lead to magnetic semiconductors with a strong quantum confinement effect [J]. *Nano Lett*, 2001, 1(10): 521–525.
- [4] MALIK M A, REVAPRASADU N, BRIEN P O. Air-stable single-source precursors for the synthesis of chalcogenide semiconductor nanoparticles [J]. *Chem Mater*, 2001, 13(3): 913–920.
- [5] JUN Y W, KOO J E, CHEON J. One-step synthesis of size tuned zinc selenide quantum dots via a temperature controlled molecular precursor approach [J]. *Chem Commun*, 2000, 20(14): 1243–1244.
- [6] HINES M A, SIONNEST P G. Bright UV-blue luminescent colloidal ZnSe nanocrystals [J]. *J Phys Chem B*, 1998, 102(19): 3655–3657.
- [7] QUINLAN F T, KUTHER J, TREMEL W, KNOLL W, RISBUD S, STROEVE P. Reverse micelle synthesis and characterization of ZnSe nanoparticles [J]. *Langmuir*, 2000, 16: 4049–4051.
- [8] HU Y, CHEN W M, CHEN J F, ZHANG Z C. Preparation of ZnS nanocrystals in network of hydrogel [J]. *Mater Lett*, 2003, 57(7): 1312–1316.
- [9] SHAO M W, LI Q, KONG L F, YU W C, QIAN Y T. The synthesis

- of hollow CdS nanospheres packed with square subunits [J]. *J Phys Chem Sol*, 2003, 64(7): 1147–1150.
- [10] HU Y, CHEN J, CHEN W, LIN X, LI X. Synthesis of novel nickel sulfide submicrometer hollow spheres [J]. *Adv Mater*, 2003, 15(9): 726–729.
- [11] ZHU J J, XU S, WANG H, ZHU J M, CHEN H Y. Sonochemical synthesis of CdSe hollow spherical assemblies via an in-Situ template route [J]. *Adv Mater*, 2003, 15(2): 156–159.
- [12] JIANG X C, XIE Y, LU J, ZHU L Y, HE W, LIU X M. Low temperature interface-mineralizing route to hollow CuS, CdS, and NiS spheres [J]. *Can J Chem*, 2002, 80(3): 263–268.
- [13] SHI W T, GAO G, XIANG L. Synthesis of ZnO whiskers via hydrothermal decomposition route [J]. *Transactions of Nonferrous Metals Society of China*, 2010, 20(6): 1049–1052.
- [14] XIONG S L, XI B J, WANG C M, XI G C, LIU X Y, QIAN Y T. Solution-phase synthesis and high photocatalytic activity of wurtzite ZnSe ultrathin nanobelts: A general route to 1D semiconductor nanostructured materials [J]. *Chem Eur J*, 2007, 13(28): 7926–7932.
- [15] PAN Z W, DAI Z R, WANG Z L. Nanobelts of semiconducting oxides [J]. *Science*, 2001, 291(5510): 1947.
- [16] FAN X M, ZHOU Z W, WANG J, TIAN K. Morphology and optical properties of tetrapod-like zinc oxide whiskers synthesized via equilibrium gas expanding method [J]. *Transactions of Nonferrous Metals Society of China*, 2011, 21(9): 2056–2060.
- [17] FENG S H, XU R R. New materials in hydrothermal synthesis [J]. *Accounts Chem Res*, 2001, 34(3): 239–247.
- [18] CAO F, SHI W D, ZHAO L J, SONG S Y, YANG J H, LEI Y Q, ZHANG H J. Hydrothermal synthesis and high photocatalytic activity of 3D wurtzite ZnSe hierarchical nanostructures [J]. *J Phys Chem C*, 2008, 112(44): 17095–17101.
- [19] HAN X, SUN J, WANG H L, DU X W, YANG J. Strong green emission from ZnSe–Ag<sub>2</sub>Se nanocomposites [J]. *J Alloy Compd*, 2010, 492(1–2): 638–641.
- [20] YI R, QIU G Z, LIU X H. Rational synthetic strategy: From ZnO nanorods to ZnS nanotubes [J]. *J Solid State Chem*, 2009, 182(10): 2791–2795.
- [21] LIANG J B, LIU J W, XIE Q, BAI S, YU W C, QIAN Y T. Hydrothermal growth and optical properties of doughnut-shaped ZnO microparticles [J]. *J Phys Chem B*, 2005, 109(19): 9463–9467.
- [22] DUAN J X, HUANG X T, WANG E K, AI H H. Synthesis of hollow ZnO microspheres by an integrated autoclave and pyrolysis process [J]. *Nanotechnology*, 2006, 17(6): 1786–1790.

## ZnSe 微球在不同水热条件下的制备与表征

段雨露<sup>1</sup>, 姚生莲<sup>1</sup>, 戴 诚<sup>1</sup>, 刘小鹤<sup>2</sup>, 徐国富<sup>1,3</sup>

1. 中南大学 材料科学与工程学院, 长沙 410083;
2. 中南大学 资源加工与生物工程学院, 长沙 410083;
3. 中南大学 有色金属材料科学与工程教育部重点实验室, 长沙 410083

**摘 要:** 以  $\text{Zn}(\text{NO}_3)_2 \cdot 6\text{H}_2\text{O}$  和  $\text{Na}_2\text{SeO}_3$  作为原料, 通过水热法制备 ZnSe 纳米晶。探讨了水热反应温度、反应时间、NaOH 浓度和  $\text{N}_2\text{H}_4 \cdot \text{H}_2\text{O}$  的添加量对最终产物的相组成、显微形貌和颗粒尺寸的影响, 并借助 XRD、SEM、TEM、PL 等测试手段对产物的相组成、显微形貌和颗粒尺寸进行表征。添加 20 mL 1 mol/L NaOH 溶液和 10 mL  $\text{N}_2\text{H}_4 \cdot \text{H}_2\text{O}$  溶液, 在 180 °C 的温度下水热反应 4 h 制备的产物主要是立方闪锌矿结构的 ZnSe 微球, 所得的 ZnSe 微球从内到外是由平均尺寸约 20 nm 的 ZnSe 纳米晶组成。结果表明: 较低的水热温度和较短的反应时间都不利于得到结晶好的纯相 ZnSe, 产物结晶性不好, 而且还会产生杂相和有较多缺陷。添加适量浓度的 NaOH 和水合肼才能确保得到形貌均匀、发光性能好的 ZnSe 微球。

**关键词:** ZnSe 微球; 纳米晶; 水热法; 发光性能

(Edited by Hua YANG)